Lipidomics Study of the Therapeutic Mechanism of Plantaginis Semen in Potassium Oxonate-Induced Hyperuricemia Rat

Wenjun Shi
Beijing University of Chinese Medicine School of Chinese Materia Medica
Fei Yang
Beijing University of Chinese Medicine School of Chinese Materia Medica
Liting Wang
Beijing University of Chinese Medicine School of Chinese Materia Medica
Nankun Qin
Beijing University of Chinese Medicine School of Chinese Materia Medica
Chengxiang Wang
Beijing University of Chinese Medicine School of Chinese Materia Medica
Guang Xu
Beijing University of Chinese Medicine School of Chinese Materia Medica
Yuying Guo
Beijing University of Chinese Medicine School of Chinese Materia Medica
Xue Yu
Beijing University of Chinese Medicine School of Traditional Chinese Medicine
Qun Ma (maqun99@163.com)
Beijing University of Chinese Medicine https://orcid.org/0000-0003-2706-9051

Research

Keywords: Hyperuricemia, lipidomics, Plantaginis semen, lipid metabolism disorder, Lowering uric acid

Posted Date: November 5th, 2020

DOI: https://doi.org/10.21203/rs.3.rs-101537/v1

Lipidomics study of the therapeutic mechanism of Plantaginis semen in potassium oxonate-induced hyperuricemia rat

Wenjun Shi[a, 1], Fei Yang[a, 1], Liting Wang[a], Nankun Qin[a], Chengxiang Wang[a], Guang Xu[a], Yuying Guo[a], Xue Yu[b], Qun Ma[a, *]

[a]School of Chinese Materia Medica, Beijing University of Chinese Medicine, Beijing 102488, China.

[b]School of Traditional Chinese Medicine, Beijing University of Chinese Medicine, Beijing 100029, China.

[1] Equal contribution.

* Corresponding authors.

Email addresses: maqun99@163.com (Qun Ma).

Tel.: +86 13910186491 (Qun Ma)

Abatract

Background

Plantaginis semen has been widely used as folk medicine and health care food against hyperuricemia (HUA) and gout, but little was known about its pharmacological mechanism.

Methods

The model was established by potassium oxonate intragastric administration. 42 Sprague-Dawley (SD) male rats were randomly divided into the control group, model group, benzbromarone group (10 mg/kg) and three Plantaginis semen groups (n = 7). The Plantaginis semen groups were treated orally with Plantaginis semen at 0.9375, 1.875 and 3.75 g/kg for 28 days. The levels of serum uric acid (UA), creatinine (Cr), triacylglycerol (TG) and tumor necrosis factor-α (TNF-α) were detected using enzyme-linked immunosorbent assay kits. Ultra performance liquid chromatography quadrupole time of flight mass spectrometry (UPLC-Q-TOF/MS) was used as the basis for serum lipidomics analysis, and orthogonal partial least squares discriminant analysis (OPLS-DA) was carried out for the pattern recognition and characteristic metabolites identification. The relative levels of critical regulatory factors of urate anion transporter 1(URAT1) and phosphatidylinositol 3-kinase/ protein kinases B (PI3K/Akt) were determined by quantitative real-time polymerase chain reaction (RT-qPCR).

Results

Compared with the model group, the levels of serum UA, Cr, and TG were significantly ($p<0.01$) decreased in benzbromarone and three Plantaginis semen groups and the level

of serum TNF-α was significantly ($p<0.05$) decreased in benzbromarone and low dose of Plantaginis semen group. With lipidomics analysis, significant lipid metabolic perturbations were observed in HUA rats, 13 metabolites were identified as potential biomarkers and glycerophospholipid metabolism pathway was mostly affected. These perturbations can be partially restored via treatment of benzbromarone and Plantaginis semen. Additionally, the URAT1 and PI3K/Akt mRNA expression levels were significantly decreased ($p<0.05$) after treatment with benzbromarone and high dose of Plantaginis semen.

Conclusions

Plantaginis semen had significant anti-HUA, anti-inflammatory and renal protection effects and could attenuate potassium oxonate-induced HUA through regulation of lipid metabolism disorder.

Trial registration

Not applicable

Key words: Hyperuricemia; lipidomics; Plantaginis semen; lipid metabolism disorder; Lowering uric acid

Background

Hyperuricemia (HUA), the cause of gout, is associated with cardiovascular diseases and metabolic diseases such as diabetes hypertension and dyslipidemia[1]. Elevated prevalent of HUA has been observed throughout the world, placing a considerable public health burden on the society[2]. Currently, two categories medicine commonly used for the treatment of HUA are uricosuric agents such as probenecid and benzbromarone and/or xanthine oxidase (XOD) inhibitors such as allopurinol[3]. However, allopurinol may produce a mild skin rash and severe cutaneous reactions and there are some unanswered questions about the pharmacological interactions of probenecid and the hepatotoxicity of benzbromarone[4, 5]. So alternative or complementary therapies are in need of reducing the risk of HUA attacks.

Traditional Chinese medicine (TCM) is an excellent representative in alternative and complementary medicine with a complete theory system and substantial herbal remedies[6]. Plantaginis semen, the dried ripe seed of Plantago asiatica L. or Plantago depressa Willd, has certain activities in anti-inflammatory, blood lipid lowering and immune regulatory actions and has been widely used as folk medicine and health care food against HUA and gout, but little was known about its pharmacological mechanism[7, 8].

It has been reported that HUA was concerned with the disorders of lipid metabolism, the results of an epidemiological survey showed that about 60% of patients with HUA had abnormal lipid metabolism and later developed HUA with hyperlipidemia[9]. However, current metabonomic studies associated with HUA are mainly pay attention

to the total relevant metabolites rather than lipids, and the lipid biomarkers should be subjected to further study[10, 11]. Lipidomics emphasis on the the determination of lipid molecular composition in cells, biofluids, tissue, or whole organism and could be a puissant tool to provide a new insight into the change of lipid metabolism in HUA and the anti-HUA mechanism of Plantaginis semen[12].

URAT1 plays a central role in renal urate reabsorption and is the target of uricosuric drugs in treating HUA[13, 14]. It has also been reported that activation of PI3K/Akt pathway is able to trigger inflammatory and kidney injuries, causing renal excretion of uric acid impaired and HUA[15-21].Both of them play an important role in the treatment of HUA.

In this study, we investigated the effects and mechanism of Plantaginis semen on HUA rats and preliminarily evaluate the actions of Plantaginis semen on URAT1 and PI3K/Akt pathway. Our findings shed light on the relationship between lipid metabolism and HUA and supplied evidences that Plantaginis semen may be used for the treatment of HUA in the clinic.

Methods

Chemicals and reagents

Benzbromarone tablets (50 mg/tablet) were provided by Excella GmbH & Co.KG (Nurnberger, Germany). Potassium oxonate was acquired from Shanghai Macklin Biochemical Co., Ltd. (Shanghai, China). Pentobarbital sodium was provided by Tianjin Fuchen Chemical Technology Co., Ltd. (Tianjin, China). LC-MS grade acetonitrile, formic acid, ammonium formate, isopropyl alcohol, methanol were

supplied by America Thermo Fisher Scientific Co., Ltd. (Massachusetts, America). Analytical grade ethanol was purchased from America Thermo Fisher Scientific Co., Ltd. (Massachusetts, America). Ultrapure water was made by America Millipore Co., Ltd. Milli-q ultra pure water machine (Massachusetts, America).

Preparation of plantaginis semen extract

Plantaginis semen was purchased from Tongrentang Chinese Medicine, (Beijing, China). 100g Plantaginis semen was taken and 65% ethanol of 8 times the amount of herbs was added to heat and reflux for 3 times, 2 h each time. The filtrate obtained from three reflux times was mixed and concentrated to 100 mL, containing crude drug content of $1.0g \cdot mL^{-1}$. The filtrate was refrigerated for later use.

Animal care and experimental design

Specific pathogen free (SPF) grade Sprague-Dawley (SD) male rats (200±20g) were bought from Vital River Laboratory Animal Technology Co., Ltd. (Beijing, China) and the certificate number is SCXK (Jing) 2016-0006. Rats were fed with a standard laboratory environment (humidity 40-70% and temperature 20-25°C) and hold on a 12 h/12 h light/dark cycle during the whole period. All experimental protocols were approved by the ethics committee of Beijing University of Chinese Medicine (Beijing, China).

After the acclimation period, rats were randomly separated out into six group equally (n=7), including control group (C), model group (M), benzbromarone group (Y), high dose group (CH), medium dose group (CM) and low dose group (CL). The rat HUA model was established by potassium oxonate intragastric administration. At 1h before

drug administration, the rats were given potassium oxonate by intragastric administration according to 1.5g•kg^{-1} dose, and the control group was given the corresponding volume distilled water by intragastric administration. Then the CH, CM, and CL groups were orally administered three dosages of Plantaginis semen (0.9375g/kg, 1.875g/kg, 3.75g/kg), and the Y group was treated with benzbromarone (10 mg/kg) once a day for 28 days.

Serum biochemical indicator measurements

On the 28th day of modeling, rats were anesthetized with 2% pentobarbital sodium (0.3 mL/100g, i.p. injection). The blood samples were taken from the abdominal aorta by a vacuum blood collection tube, and centrifuged for 10 min (3000 rpm, 10°C). Serum samples were stored at -80°C for analysis. The levels of serum UA, Cr, TG and TNF-α were measured using commercially available kits (Jiancheng, Nanjing, China) according to the manufacturer's instructions.

Serum UPLC-Q-TOF/MS analysis

Serum samples were thawed at room temperature before data acquisition. 320 μL of chloroform-methanol (3:1, V/V) was put into 80μL serum sample, vortex for 15s each time and centrifuged (10000 r•min^{-1}) at room temperature for 10 min. The supernatant was taken for UPLC−Q-TOF/MS analysis.

The UPLC column was Acquity CSH C18(2.1×100mm,1.7μm, Waters Corp., Milford, MA, USA) with the column temperature maintained at 40 °C, flow rate 0.3mL•min^{-1}. The gradient mobile phase was composed of acetonitrile-water-formic acid (60:40:0.1) plus 10mmol·L^{-1} ammonium formate (phase A) and isopropanol-methanol-formic acid

155 (90:10:0.1) plus 10mmol·L^{-1} ammonium formate (phase B). The gradient elution
156 programme was as follows: 0.0min, 60%A; 0.0~3.1min, 57%A; 3.1~4.1min, 30%A;
157 4.1~4.3min, 27%A; 4.3~8.0min, 23%A; 8.0~10.0 min, 60%A.
158 MS analysis was performed by Xevo G2 Q/TOF MS (Waters Corp., Milford, MA, USA)
159 system. The optimized mass conditions were as follows: the ionization mode is
160 electrospray ionization and was set in positive modes. The flow rate of the cone gas
161 was 20 L/h. The capillary voltage was 2.5 kV in positive mode. The source temperature
162 was 120 °C and the atomizing gas temperature is 450°C. MS data were collected in the
163 full scan mode from m/z50–1200 amu.
164 **Data processing**
165 The raw data obtained by UPLC-Q/TOF-MS were imported into MassLynx
166 V4.1software (Waters Corp., Milford, MA, USA) to pretreat the data, including peak
167 filtering and peak alignment. The resultant data matrices were introduced to SIMCA-P
168 (version 13.0, Umetrics, Sweden) for orthogonal projection to latent structures (OPLS)
169 analysis. The multivariate analysis results are expressed in the form of scores plot and
170 S-plot to observe the global clustering trends of various groups and visualize their
171 distributions. The model parameters including R^2 (goodness of fit) and Q^2 (goodness of
172 prediction) calculated from the OPLS-DA models were used to evaluate the quality of
173 these models. Finally, potential biomarkers were filtered by the results of variable
174 importance for the projection (VIP) values (VIP>1) and t-test ($p<0.5$) values. The
175 above-mentioned biomarkers are analyzed by m/z, retention time (RT) and fragment
176 ion information, combined with HMDB (http://www.hmdb.ca/) and Lipid Maps

(http://www.lipidmaps.org) database to confirm differential metabolites.

Finally, the pathway analysis of potential biomarkers were performed with the Metabo Analyst (http://www.metaboanalyst.ca/), which was based on the database source including KEGG (http://www. genome. jp/kegg/) and a correlation metabolic networks for disturbed pathways in HUA rats was constructed.

RT-qPCR

RNA from kidney tissue was extracted by Hipure Total RNA Mini Kit (Magen, Guangzhou, China). RT-qPCR was carried out using TB Green Primix Ex TaqII kit (Takara, Kyoto-fu, Japan) in Bio-Rad CFX96 Real Time PCR System (BIO-RAD, Shanghai, China). The primers used in the study are: URAT1, Forward: 5'-CTCTGCTGGTGTATGGAGTGG-3', Reverse: 5'-TTTCTGGATGTCTTGGATGGT-3', PI3K, Forward:5'-GGTTCTTGCGAAGTGAGATAGCCC-3, Reverse:5'-ACCTGCTGCGTGAAGTCCTGTA-3', Akt, Forward:5'-TGTCTCGTGAGCGCGTGTTTT-3', Reverse:5'-CCGTTATCTTGATGTGCCCGTC-3'. Ct (cycle threshold) value was collected. Detected in triplicate and the relative expression levels of genes were determined by the $2^{-\triangle\triangle Ct}$ method.

Results

Plantaginis semen decreased the level of serum UA in HUA rats

After 28 days, rats fed potassium oxonate change in the lever of serum UA (Fig.1a). As compared to the C group (92.84 ± 16.22 umol•L^{-1}), the lever of serum UA in the M group (186.44 ± 26.20 umol•L^{-1}) increased significantly ($p<0.01$), which represents the success of the mold. Conversely, the lever of serum UA in the Y (138.91 ± 15.41

umol•L^{-1}), CH (149.44 ± 21.12 umol•L^{-1}), CM (159.11 ± 9.78 umol•L-1) and CL (145.85 ± 6.81 umol•L^{-1}) groups all significantly ($p<0.01$) reduced, compared to the case for the M group. These results indicated that Plantaginis semen could effectively lower serum uric acid lever.

Plantaginis semen exerted renal protection effect in HUA rats

Serum Cr is necessary to assess kidney function and can reflect the extent of renal injury[22]. The results depicted in Fig.1b show that the levels of serum Cr (45.79 ± 4.02μmol•L^{-1}) in the M group were significantly ($p<0.01$) increased, as compared to serum Cr (35.28 ± 7.26μmol•L^{-1}) observed for the C group. After receiving treatment for 28 days, the serum Cr levels (35.47±3.51, 39.72±5.55, 39.02±4.27μmol•L^{-1}) in the CH, CM and CL groups were significantly ($p<0.01$) reduced, as compared to that of the M group. And the serum Cr of these 3 groups all lower than Y group, indicated that Plantaginis semen has a good protective effect on renal.

Plantaginis semen ameliorated serum TG accumulation in HUA rats

Serum level of TG was remarkably ($p<0.01$) elevation in the M group as compared with the control group. Then, over 28 days of treatment, the TG levels in the CH (0.18 ± 0.08 mmol/L), CM (0.17 ± 0.07 mmol/L), and CL (0.24 ± 0.06 mmol/L) groups all significantly ($p<0.01$) reduced compared to that in the M group (0.50 ± 0.17 mmol/L). The results were depicted in Fig.1c. The effect of CL group was close to that of Y group, and the effects of CM and CH group were better than Y and CL group and close to C group.

Plantaginis semen reduced the level of TNF-α in HUA rats

In our study, the levels of TNF-α in the serum were used to evaluate the anti-inflammatory effect of Plantaginis semen in vivo. As shown in Fig.1d, the level of TNF-α in the M group (117.10 ± 27.03 pg•mL^{-1}) significantly ($p<0.05$) higher than that in the C group (81.77 ± 17.08 pg•mL^{-1}). In the CL group, the level of TNF-α (85.30 ± 21.29 pg•mL^{-1}) was significantly (*$p<0.05$*) decreased compared to M group and are nearly to Y group (81.77 ± 17.08 pg•mL^{-1}). The levels of TNF-α in the CM and CH groups decreased but remained insignificant.

Metabolic perturbations and differential metabolites associated with HUA Rats

To investigate the effect of potassium oxonate on endogenous component changes, an OPLS-DA model was used to compare the serum samples obtained during 28 days from the model and control groups. As shown in the OPLS-DA score plots of serum samples (Fig.2a), a separation between the model group and the control group was clearly seen, indicating that the HUA model was successful and had completely different metabolic profiles compared with the healthy controls. The parameters of the OPLS-DA models were as follows: R^2Y=0.936 and Q^2= 0.737. The R^2Y and Q^2 values reflect excellent predictability and explain the differences between the control and model groups. In addition, 200-iteration permutation tests were also performed to assess the robustness of OPLS-DA models (Fig.2b). The validation plots showed that the original OPLS-DA models were not random and overfitted as both permutated Q^2 and R^2 values were lower than the corresponding original values along with the Y-intercepts of the regression lines of the Q^2-points below zero.

Potential biomarkers were identified from the interactions between control and model

groups using the corresponding S-plot analysis under OPLS-DA model. The metabolites whose VIP values>1 and p values<0.05 of OPLS-DA were presumed as significant differences. Databases such as KEGG, METLIN, and HMDB were used to identify potential bio-markers, along with UPLC/Q-TOF-MS information. The results were shown in table 1. 13 metabolites were matched and identified, including 4 phosphatidylcholine (PC), 4 hemolytic phosphatidylcholine (LPC), 2 phosphatidylethanolamine (PE), 2 TG, 1 cholesterol ester (CE). Compared with the control group, the metabolic perturbations occurring in serum of the HUA rats were mainly characterized by increased levels of these lipids.

Table 1 Identification results of differential metabolites associated with HUA rats

No.	RT(min)	*m/z*	Formula	Metabolite	VIP	M vs. C	Y vs. M	CL vs. M	CM vs. M	CH vs. M
1	5.5875	898.7862	$C_{57}H_{100}O_6$	TG(18:2/18:1/18:2)	2.75	↑**	↓##	—	↓##	↓##
2	8.9231	931.7526	$C_{55}H_{92}O_6$	TG(20:4/14:0/18:3)	2.55	↑**	↓#	—	↓##	—
3	8.4467	925.7098	$C_{48}H_{92}NO_8P$	PC(24:1/16:1)	2.54	↑**	↓#	—	↓##	↓##
4	2.6081	496.3364	$C_{50}H_{94}NO_8P$	PC(24:1/18:2)	2.43	↑**	—	↓##	↓##	↓##
5	9.0509	264.9627	$C_{41}H_{82}NO_8P$	PC(15:0/18:0)	2.29	↑**	—	—	↓##	—
6	9.0937	326.9082	$C_{54}H_{102}NO_8P$	PC(24:1/22:2)	2.70	↑**	↓##	↓##	↓##	↓##
7	1.8681	516.3129	$C_{24}H_{48}NO_7P$	LPC(16:1/0:0)	2.35	↑**	—	↓#	—	—
8	2.0389	610.3188	$C_{30}H_{54}NO_7P$	LPC(22:4/0:0)	2.56	↑**	↓##	↓##	—	—
9	2.0460	542.3279	$C_{26}H_{50}NO_7P$	LPC(18:2/0:0)	2.37	↑**	↓##	↓##	↓#	—

10	4.1085	273.6606	$C_{26}H_{54}NO_7P$	LPC(18:0/0:0)	2.09	↑**	—	—	↓#	—
11	9.3573	416.2983	$C_{45}H_{76}NO_8P$	PE(18:3/22:4)	2.15	↑**	—	—	↓#	—
12	9.0937	326.9082	$C_{53}H_{102}NO_8P$	PE(24:1/24:1)	2.43	↑**	↓##	↓##	↓##	↓##
13	9.0230	376.8943	$C_{51}H_{90}O_2$	CE(24:1)	2.60	↑**	↓##	↓##	↓##	↓##

C, control group; M, model group; Y, benzbromarone group; CL, low dosage group; CM, medium dosage group; CH, high dosage group; **, $p<0.01$ vs. control group. *, $p<0.05$ vs. control group; ##, $p<0.01$ vs. model group; #, $p<0.05$ vs. model group. (↑): up-regulated and (↓): down-regulated. (-):no statistically significant difference

Metabolic changes under the treatment of benzbromarone and Plantaginis semen

Fig.3 showed distinct metabolic profiles among different groups and there is a tendency to return to the normal group in benzbromarone-treated and different dose Plantaginis semen-treated groups. Heatmap analysis was produced to intuitively compare the relative content of 13 potential metabolites among 6 groups referring to table1 (Fig.4). Control group and model group clearly distinguished, the color depth of benzbromarone group and Plantaginis semen groups were close to control group, indicating that the performance on the callback of these metabolites is extraordinary obvious. 8, 7, 11 and 6 differential metabolites associated with HUA in serum of rats were significantly ($p<0.05$) reversed by benzbromarone, low dose Plantaginis semen, medium dose Plantaginis semen, high dose Plantaginis semen respectively (Fig.5). These findings suggested that the metabolic perturbations induced by HUA could be normalized by benzbromarone and Plantaginis semen treatment. Among them, the effect of normalizing differential metabolites in the middle dose Plantaginis semen group was

271 the best.

272 **Metabolic pathways related to potential biomarker**

273 The 13 potential biomarkers were found to be primarily involved in 6 disturbed
274 metabolic pathways. Based on the impact value greater than 0.1 and p value less than
275 0.05, glycerophospholipid metabolism was considered as the most relevant pathways
276 in potassium oxonate-induced HUA (Fig.6) and a global metabolic network was
277 mapped (Fig.7).

278 **Plantaginis semen downregulated the mRNA expression of PI3k, Akt, URAT1 in**
279 **HUA rats**

280 The mRNA expressions of PI3K, Akt and URAT1 in rat renal were shown in Fig.8. The
281 contents of URAT1 and PI3K/Akt were significantly ($P<0.05$) increased in M group
282 compared with those in C group. After 28 days administration, Y group and three
283 Plantaginis semen groups all showed significantly ($P<0.01$) decrease in the expressions
284 of URAT1 mRNA, while there were no significant differences ($P>0.05$) in the
285 expressions of PI3K and Akt mRNA between M, CL and CM groups. The Akt
286 expression of CH group was approximate to that of Y group and the PI3k expression of
287 CH group was even lower than Y group (Fig.8 b, c).

288 **Discussion**

289 The study provides evidences that Plantaginis semen attenuates potassium oxonate-
290 induced HUA through regulation of lipid metabolism disorder. This study also presents
291 the change in lipid metabolism of HUA which helps to explain the relationship between
292 lipid metabolism and HUA. Further, Plantaginis semen influenced URAT1 and

PI3K/Akt pathway to support its UA lowing efficacy in HUA rats.

Urate crystals deposit in the blood vessel walls and kidneys will cause chronic inflammatory damage and releasing large amounts of inflammatory factors, such as TNF-α, IL-6[23]. Elevated TNF-α levels will also further aggravate renal tubular and interstitial damage, resulting in UA excretion impaired[24, 25]. So long-term persistent HUA is closely related to inflammation and will lead to renal dysfunction and renal impairment[13].In this experiment, by determining the levels of serum Cr, UA and serum TNF-α, we can evaluate the renal function of HUA rats and asses the anti-inflammatory and reducing uric acid effects of Plantaginis semen. While increasing the serum UA of the rats, the levels of serum TNF-α and Cr also increased, indicating that inflammatory factors are involved in the development and progression of HUA[26] and HUA rats had renal function injury and chronic low-grade inflammatory in a state of high uric acid. However, different dose of Plantaginis semen treatment could significantly decrease the levers of serum UA in HUA rats and reduce their serum Cr and TNF-α concentration simultaneously, indicating that the ethanol extract of Plantaginis semen could improve the renal injury and protect renal in HUA rats and may treat HUA via their anti-inflammatory effect.

The link between HUA and metabolic syndrome had been recognized, and a growing body of research indicated that there is a strong concurrence between dyslipidemia and hyperuricemia. Studies have indicated that elevated levels of SUA up regulates the concentration of TG[27]. Benzbromarone can regulate the expression of lipid metabolism genes, when benzbromarone was used in uric acid-lowering therapy on

315 hypercholesterolem and hypertriglyceridemia in gouty patients, the lever of TG
316 modestly decreased[28, 29]. The level of serum UA increased accompanied with the
317 increment of serum TG levels indicating that disorders of lipid metabolism occurred in
318 HUA rats. After the treatment with benzbromarone and Plantaginis semen, the serum
319 TG level was decreased which demonstrated that Plantaginis semen has similar effect
320 to benzbromarone and the Plantaginis semen may via lowering accumulation of lipids
321 and restoring lipid metabolism to ease HUA.
322 A lipidomics approach was also applied to describe the metabolic differences in this
323 experiment. In our study, HUA rats in our study exhibited an elevated level of CEs, TGs,
324 PCs, LPCs, PEs in serum compared with normal rat. CE (24:1) is a kind of cholesterol
325 fatty acid ester and can be hydrolyzed by cholesterol esterase to produce cholesterol
326 and free fatty acids[30]. Therefore, the increase of CE level will lead to the increase of
327 serum total cholesterol (TC). Elevated serum TC is more common in nephrotic
328 syndrome and cardiovascular and cerebrovascular diseases and the determination of
329 serum TC has become a routine item for the analysis of blood lipids[31]. The serum CE
330 level in HUA rats increased, indicating the occurrence of dyslipidemia. The synthesis
331 of TG will need NADPH and produce uric acid[32], the increase of serum uric acid
332 provides raw materials for TG synthesis, HUA maybe a causal factor for high TG, and
333 the lipidomics result was consistent with the literature reports [33, 34]. LPCs are
334 metabolites of PCs. LPC is an important lipid compound on oxidized low-density
335 lipoprotein (ox-LDL), serum LDL cholesterol was positively correlated with uric acid
336 levels[35]. Liu Ning et al. found that UA could activate the phospholipid-remodeling

enzymes LPCAT3 and LXRα in vivo and in vitro, and LPCAT3 possesses primary LPC acyltransferase activity and catalyzes the production of PCs[36], so the levels of PC and LPC were both up-regulated in HUA rats. PE is an early indicators for the risk of atherogenesis[37], and high serum UA levels have an independent association with increased arterial stiffness[38], the elevated serum PE level may be an intermediate process of hyperuricemia leading to atherosclerosis.

Glycerophospholipid metabolism was considered as the most relevant pathways in potassium oxonate-induced HUA. Glycerophosphatide is one of the most abundant phospholipids in the body. It is also one of the components of bile and membrane surfactant besides biofilm[39]. TG, PC, LPC and PE were mainly involved in glycerophospholipids metabolism and their levels were obviously increased in the serum of the HUA rats indicating glycerophospholipid plays a crucial role in the development of HUA and high uric acid will induce phospholipids metabolic disturbances. The results of lipidomics indicated that lipid metabolism disorder occurred in HUA rats, whereas, the change was reversed under the Plantaginis semen treatment. From a holistic perspective, variations in the metabolite profiles of different groups showed that Plantaginis semen could enhance the metabolism of endogenous substances in HUA rats, which may be the potential mechanism of Plantaginis semen in the treatment of HUA.

Plantaginis semen significantly inhibited the expression of URAT1 in the renal tissue of HUA rats, indicating that Plantaginis semen could achieve the effect of treating HUA by promoting uric acid excretion. PI3K/Akt pathway is closely related to

inflammation[15, 40, 41], the inhibitory effect of Plantaginis semen on PI3k/Akt pathway indicated that the mechanism of protecting kidney and reducing serum UA may be related to its anti-inflammatory response. Huang Wenhui et al. found that the PI3K/Akt signaling pathway could regulate the expression of URAT1[42]. In this study, we also found that renal URAT1 mRNA, PI3K mRNA and Akt mRNA in the CH group showed a downregulation trend. It was speculated that Plantaginis semen mediated the PI3K/Akt signaling pathway to regulate the expression of URAT1. However, there were still some deficiencies in this study, and the relationship between PI3K/Akt and URAT1 needed to be further verified.

Conclusions

Plantaginis semen had uric acid reduction, anti-inflammatory, kidney protection and lipid-lowering pharmacological effects and a promising drug to treat HUA. 13 endogenic compounds were identified as HUA biomarkers. The mechanism of Plantaginis semen treating HUA might be attributed to its regulation of lipid metabolism disorder especially the regulation of glycerophospholipid metabolism pathway. In addition, Plantaginis semen may down-regulate URAT1 expression by inhibiting the PI3K/Akt pathway, but the mechanism needs to be further studied.

Figure legends:

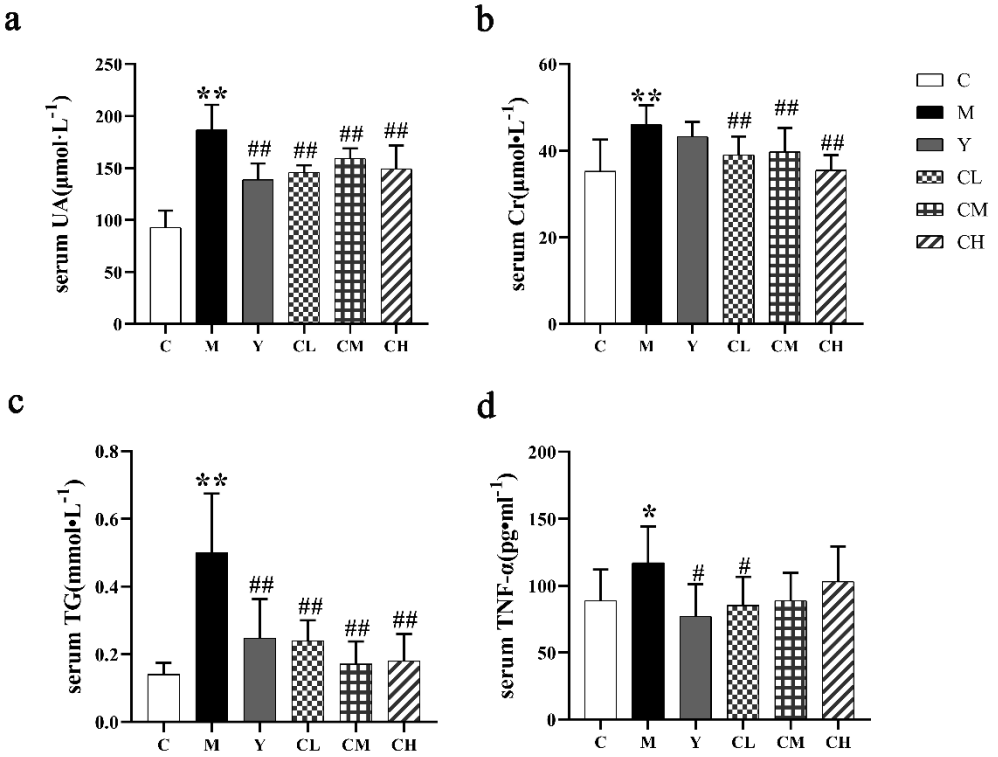

Fig. 1 The levels of serum UA, Cr, TG, TNF-α in each group. C, control group; M, model group; Y, benzbromarone group; CL, low dosage group; CM, medium dosage group; CH, high dosage group; values are given as the mean ± SD (n=7), **, P<0.01 vs. control group. *, P<0.05 vs. control group; ##, P<0.01 vs. model group; #, P<0.05 vs. model group.

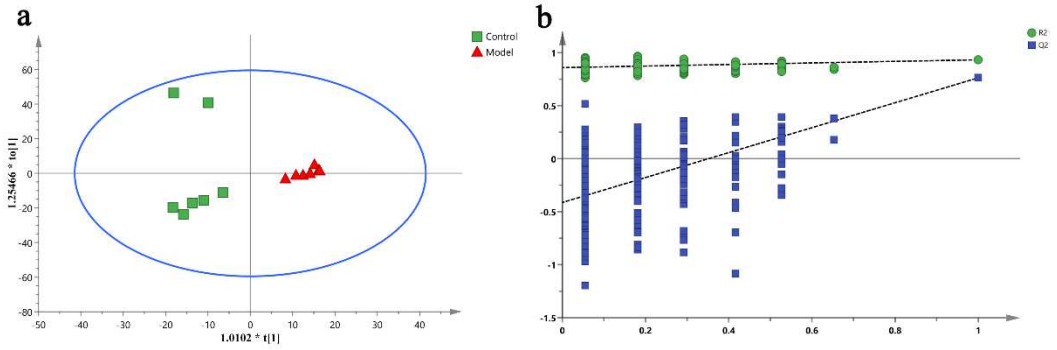

Fig. 2 OPLS-DA score plots (a) and the corresponding validation plots (b) with 200 times permutation tests obtained.

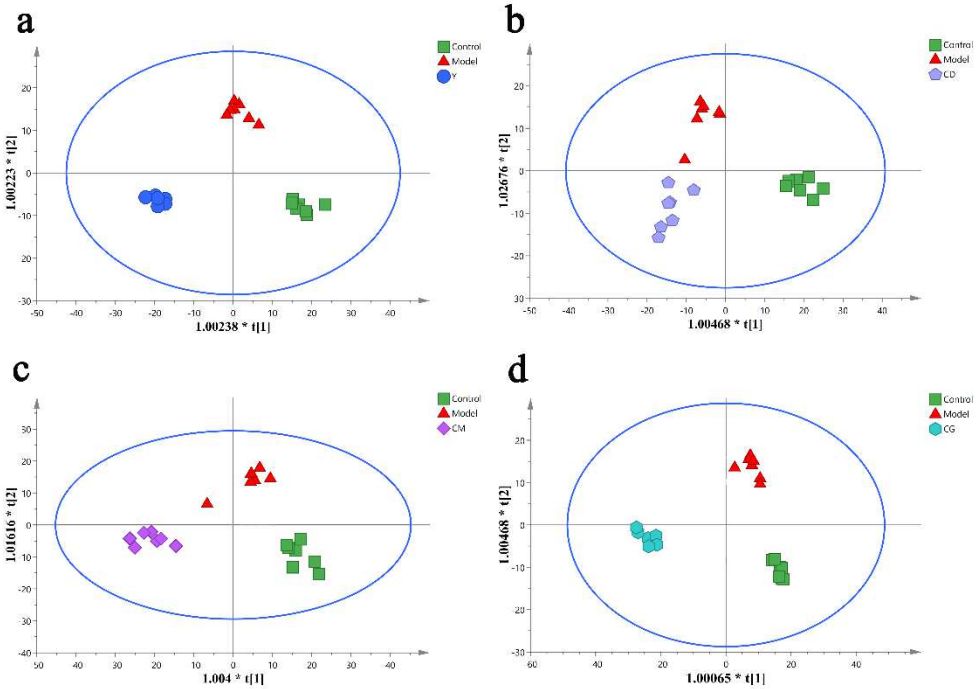

Fig. 3 Metabolic profiles of rat serum in the control, model, benzbromarone, and different dose Plantaginis semen groups. C, control group; M, model group; Y, benzbromarone group; CL, low dosage group; CM, medium dosage group; CH, high dosage group.

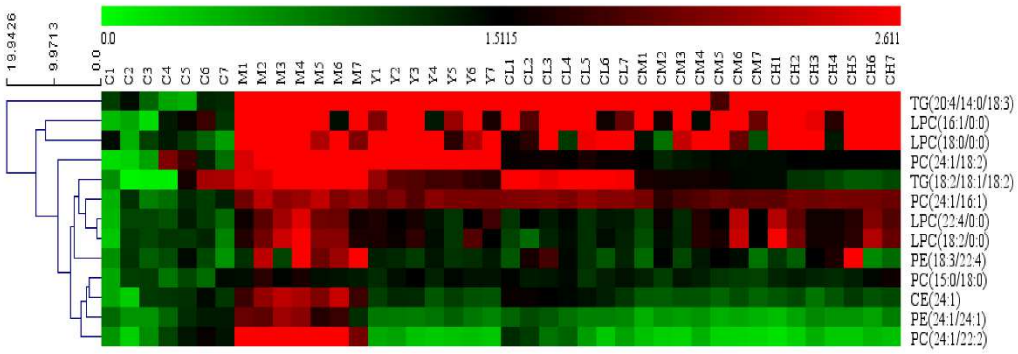

Fig. 4 Heat map analysis of relative contents of potential metabolites. (green through dark red corresponding to a progressive increase in concentration). C, control group; M, model group; Y, benzbromarone group; CL, low dosage group; CM, medium dosage group; CH, high dosage group.

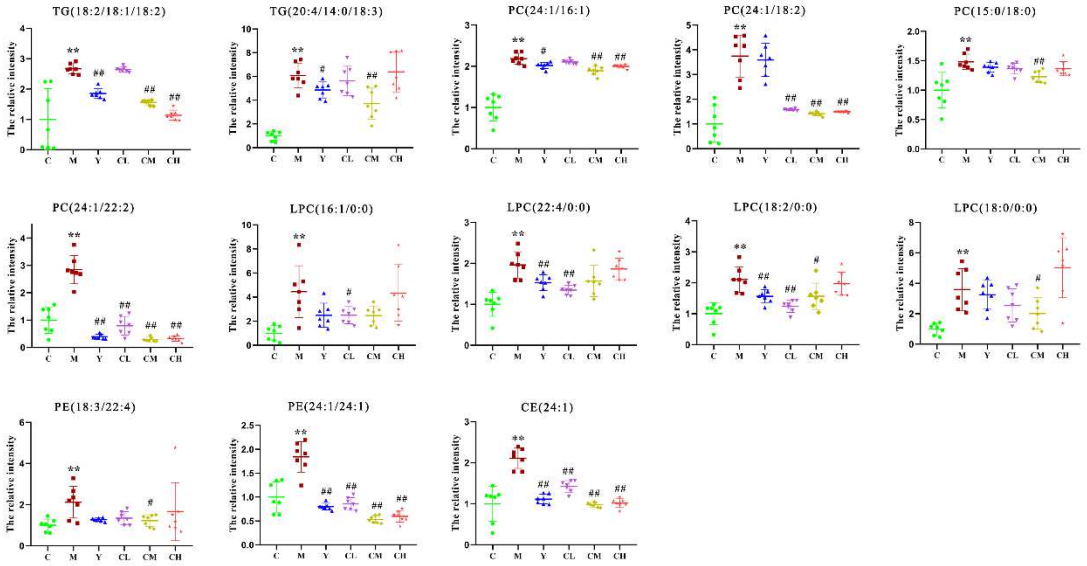

401

402 **Fig. 5** Comparison of 13 biomarkers peak relative signal intensities in 6 groups. The

403 relative value of potential biomarkers in the control group was set as 1. C, control group;

404 M, model group; Y, benzbromarone group; CL, low dosage group; CM, medium dosage

405 group; CH, high dosage group; **, P<0.01 vs. control group. *, P<0.05 vs. control

406 group; ##, P<0.01 vs. model group; #, P<0.05 vs. model group.

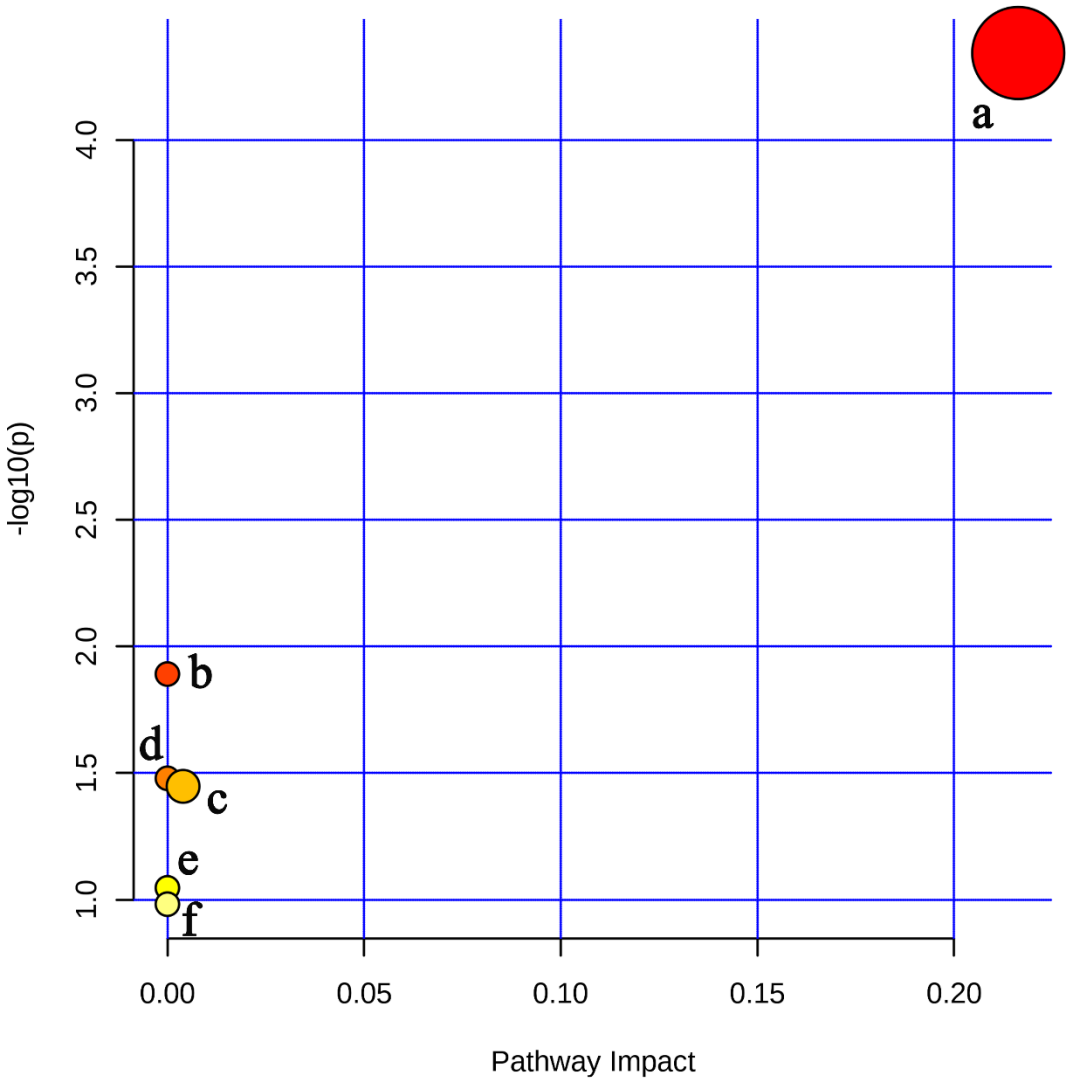

Fig. 6 six pathway related to changed biomarkers. a: Glycerophospholipid metabolism, b: Linoleic acid metabolism, c: Glycosylphosphatidylinositol (GPI)-anchor biosynthesis, d: alpha-Linolenic acid metabolism, e: Arachidonic acid metabolism, f: Steroid biosynthesis.

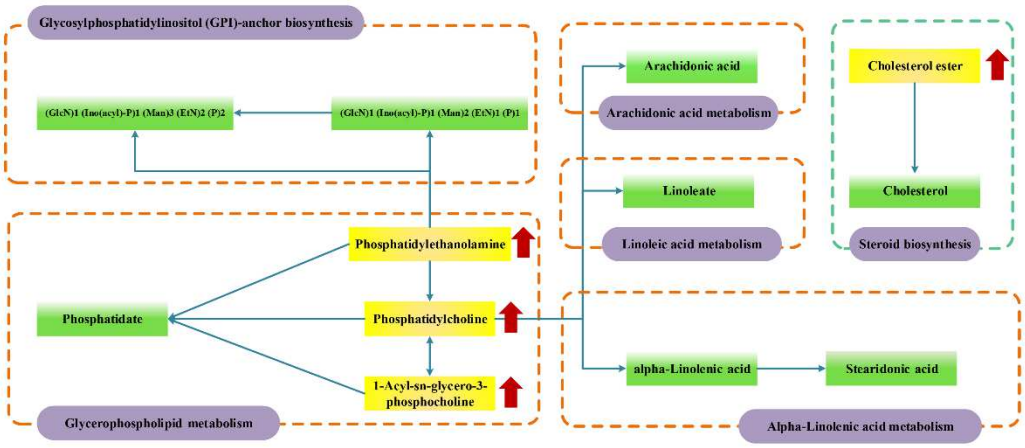

412

413 **Fig. 7** KEGG global metabolic network related to changed biomarkers. The purple
414 textboxes represented the pathways, the yellow and green textboxes represented the
415 significant and no detection metabolites. The arrows in red represented the up regulated
416 metabolites. The arrows in blue represented direct or indirect connections between two
417 metabolites.

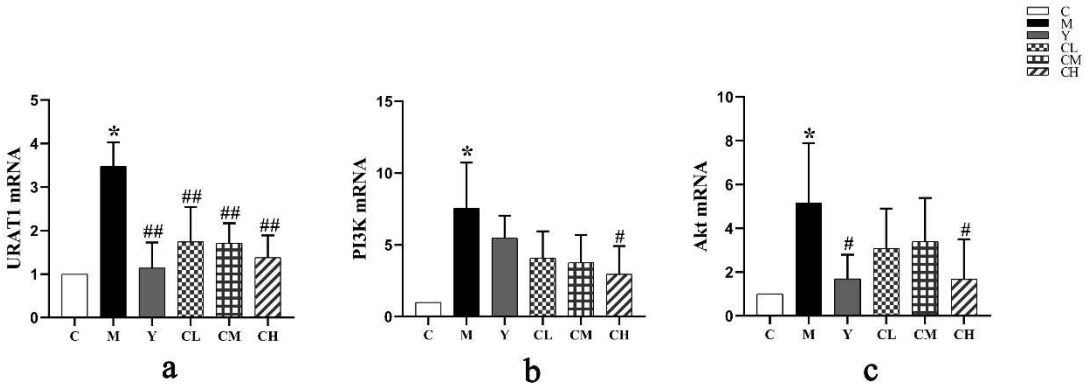

418

419 **Fig. 8** Effects of Plantaginis semen on PI3k/Akt and UTAR1 mRNA expression. C,
420 control group; M, model group; Y, benzbromarone group; CL, low dosage group; CM,
421 medium dosage group; CH, high dosage group; values are given as the mean ± SD(n=7),
422 **, P<0.01 vs. control group. *, P<0.05 vs. control group; ##, P<0.01 vs. model group;
423 #, P<0.05 vs. model group.

List of abbreviations

CE: Cholesterol ester

Cr: Creatinine

HUA: Hyperuricemia

LPC: Hemolytic phosphatidylcholine

UA: Uric acid

UPLC−Q-TOF/MS: ultra performance liquid chromatography quadrupole time of flight mass spectrometry

OPLS-DA: Orthogonal partial least squares discriminant analysis

Ox-LDL: Oxidized low-density lipoprotein

PC: Phosphatidylcholine

PE: Phosphatidylethanolamine

PI3K/Akt: Phosphatidylinositol 3-kinase/ protein kinases B

Retention time: RT

RT-qPCR: Quantitative real-time polymerase chain reaction

SPF: Specific pathogen free

SD: Sprague-Dawley

TCM: Traditional Chinese medicine

TG: Triacylglycerol

TC: Total cholesterol

TNF-α: Tumor necrosis factor-α

URAT1: urate anion transporter 1

VIP: Variable importance in the projection

XOD: xanthine oxidase

Declarations

Ethics approval and consent to participate

The experimental protocol was approved by the ethics committee of Beijing University of Chinese Medicine (Beijing, China).

Consent for publication

Not applicable

Availability of data and materials

The datasets used and/or analysed during the current study are available from the corresponding author on reasonable request.

Competing interests

The authors declare that they have no competing interests.

Funding

This research was supported by school-level vertical development funding of Beijing University of Chinese Medicine (Beijing, China).

Authors' contributions

FY and XY established hyperuricemia rat model and collected serum samples. LTW collected serum samples and measured serum biochemical indicators. NKQ collected and analyzed UPLC-Q-TOF/MS data. CXW used simca-p software for OPLS-DA analysis. YYG found and identified differential metabolites. GX conducted metabolic pathway enrichment analysis. WJS performed the RT-PCR examination of the kidney,

and was a major contributor in writing the manuscript. QM conducted trial design and guidance. All authors have read and approved the final manuscript.

Acknowledgements

None

Authors' information

Wenjun Shi and Fei Yang contributed equally to this work.

Affiliations

School of Chinese Materia Medica, Beijing University of Chinese Medicine, Beijing, 102488, China

Wenjun Shi, Fei Yang, Nankun Qin, Chengxiang Wang, Guang Xu, Yuying Guo & Qun Ma.

School of Traditional Chinese Medicine, Beijing University of Chinese Medicine, Beijing 100029, China.

Xue Yu.

Corresponding author

Correspondence to Qun Ma.

Referances

1. Dalbeth N, Merriman TR, Stamp LK. Gout. Lancet. 2016; 388:2039-2052.

2. Smith E, March L: Global Prevalence of Hyperuricemia. A Systematic Review of Population-Based Epidemiological Studies. Arthritis & Rheumatology. 2015; 67:3.

3. Otani N, Ouchi M, Kudo H, Tsuruoka S, Hisatome I, Anzai N. Recent approaches

to gout drug discovery: an update. Expert Opin Drug Discov. 2020; 15:943-954.

4. Strilchuk L, Fogacci F, Cicero AF. Safety and tolerability of available urate-lowering drugs: a critical review. Expert Opin Drug Saf. 2019; 18:261-271.

5. Stamp LK, Haslett J, Frampton C, White D, Gardner D, Stebbings S, Taylor G, Grainger R, Kumar R, Kumar S, et al. The safety and efficacy of benzbromarone in gout in Aotearoa New Zealand. Intern Med J. 2016; 46:1075-1080.

6. Pan Y, Kong LD. High fructose diet-induced metabolic syndrome: Pathophysiological mechanism and treatment by traditional Chinese medicine. Pharmacol Res. 2018; 130:438-450.

7. Zhang XY, Cheng J, Zhao P, Chen KL, Li J. Screening the Best Compatibility of Selaginella moellendorffii Prescription on Hyperuricemia and Gouty Arthritis and Its Mechanism. Evid Based Complement Alternat Med. 2019; 10.1155/2019/7263034.

8. Sun X, Lan J, Tong R, Zhang H, Sun S, Xiong A, Wang Z, Yang L. An integrative investigation on the efficacy of Plantaginis semen based on UPLC-QTOF-MS metabolomics approach in hyperlipidemic mice. Biomed Pharmacother. 2019; 10.1016/j.biopha.2019.108907.

9. Guo LF, Chen X, Lei SS, Li B, Zhang NY, Ge HZ, Yang K, Lv GY, Chen SH. Effects and Mechanisms of Dendrobium officinalis Six Nostrum for Treatment of Hyperuricemia with Hyperlipidemia. Evid Based Complement Alternat Med. 2020; 10.1155/2020/2914019.

10. Huang CC, Lou BS, Hsu FL, Hou CC. Use of urinary metabolomics to evaluate

the effect of hyperuricemia on the kidney. Food Chem Toxicol. 2014; 74:35-44.

11. Zhang Y, Zhang H, Chang D, Guo F, Pan H, Yang Y. Metabolomics approach by (1)H NMR spectroscopy of serum reveals progression axes for asymptomatic hyperuricemia and gout. Arthritis Res Ther. 2018; 20:111.

12. Alex Brown H. Lipidomics: when apocrypha becomes canonical. Curr Opin Chem Biol. 2012; 16:221-226.

13. Xu L, Shi Y, Zhuang S, Liu N. Recent advances on uric acid transporters. Oncotarget. 2017; 8:100852-100862.

14. Terkeltaub R, Bushinsky DA, Becker MA. Recent developments in our understanding of the renal basis of hyperuricemia and the development of novel antihyperuricemic therapeutics. Arthritis Res Ther 2006; 8 Suppl 1:S4.

15. Wullschleger S, Loewith R, Hall MN. TOR signaling in growth and metabolism. Cell. 2006; 124:471-484.

16. Braga TT, Foresto-Neto O, Camara NOS. The role of uric acid in inflammasome-mediated kidney injury. Curr Opin Nephrol Hypertens. 2020; 29:423-431.

17. Chen MQ, Wang HY, Shi WR, Sun YX. Estimate of prevalent hyperuricemia by systemic inflammation response index: results from a rural Chinese population. Postgrad Med. 2020; doi: 10.1080/00325481.2020.1809870..

18. Dragoș D, Manea MM, Timofte D, Ionescu D. Mechanisms of Herbal Nephroprotection in diabetes mellitus. J Diabetes Res. 2020; doi: 10.1155/2020/5710513.

19. Wang K, Zhang Y, Cao Y, Shi Z, Lin Y, Chen Y, Zhao H, Liu X. Glycyrrhetinic acid

534 alleviates acute lung injury by PI3K/AKT suppressing macrophagic Nlrp3
535 inflammasome activation. Biochem Biophys Res Commun. 2020; 532(4):555-
536 562.
537 20. Dos Santos M, Veronese FV, Moresco RN. Uric acid and kidney damage in
538 systemic lupus erythematosus. Clin Chim Acta. 2020; 508:197-205.
539 21. Wang Y, Chen C, Yan Y, Yuan Y, Wang KK, Chu C, Hu JW, Ma Q, Liao YY, Fu BW, et
540 al. Association of uric acid in serum and urine with subclinical renal damage:
541 Hanzhong Adolescent Hypertension Study. PLoS One. 2019; 14(11):e0224680.
542 22. Moore JF, Sharer JD. Methods for Quantitative Creatinine Determination. Curr
543 Protoc Hum Genet. 2017; 93:A.3o.1-a.3o.7.
544 23. Luis-Rodríguez D, Donate-Correa J, Martín-Núñez E, Ferri C, Tagua VG, Pérez
545 Castro A, Mora-Fernández C, Navarro-González JF. Serum urate is related to
546 subclinical inflammation in asymptomatic hyperuricaemia. Rheumatology
547 (Oxford). 2020; doi: 10.1093/rheumatology/keaa425.
548 24. Adachi T, Arito M, Suematsu N, Kamijo-Ikemori A, Omoteyama K, Sato T,
549 Kurokawa MS, Okamoto K, Kimura K, Shibagaki Y, Kato T. Roles of layilin in TNF-
550 α-induced epithelial-mesenchymal transformation of renal tubular epithelial
551 cells. Biochem Biophys Res Commun. 2015; 467:63-69.
552 25. Xu D, Lv Q, Wang X, Cui X, Zhao P, Yang X, Liu X, Yang W, Yang G, Wang G, et al.
553 Hyperuricemia is associated with impaired intestinal permeability in mice. Am
554 J Physiol Gastrointest Liver Physiol. 2019; 317:G484-g492.
555 26. Isaka Y, Takabatake Y, Takahashi A, Saitoh T, Yoshimori T. Hyperuricemia-

induced inflammasome and kidney diseases. Nephrol Dial Transplant. 2016; 31:890-896.

27. Lippi G, Montagnana M, Luca Salvagno G, Targher G, Cesare Guidi G. Epidemiological association between uric acid concentration in plasma, lipoprotein(a), and the traditional lipid profile. Clin Cardiol. 2010; 33:E76-80.

28. Tutal E, Sayın B, Ertugrul DT, Ibis A, Sezer S, Ozdemir N. Is there a link between hyperuricemia, morning blood pressure surge, and non-dipping blood pressure pattern in metabolic syndrome patients? Int J Nephrol Renovasc Dis. 2013; 6:71-77.

29. Cai HY, Wang T, Zhao JC, Sun P, Yan GR, Ding HP, Li YX, Wang HY, Zhu WL, Chen KX. Benzbromarone, an old uricosuric drug, inhibits human fatty acid binding protein 4 in vitro and lowers the blood glucose level in db/db mice. Acta Pharmacol Sin. 2013; 34:1397-1402.

30. Tan Y, Liu X, Zhou K, He X, Lu C, He B, Niu X, Xiao C, Xu G, Bian Z, et al. The Potential Biomarkers to Identify the Development of Steatosis in Hyperuricemia. PLoS One. 2016; 11:e0149043.

31. Tao M, Wang HP, Sun J, Tian J. Progress of research on dyslipidemia accompanied by nephrotic syndrome. Chronic Dis Transl Med. 2020; 6:182-187.

32. Gu Q, Hu X, Meng J, Ge J, Wang SJ, Liu XZ. Associations of Triglyceride-Glucose Index and Its Derivatives with Hyperuricemia Risk: A Cohort Study in Chinese General Population. Int J Endocrinol. 2020; 2020:3214716.

33. Peng TC, Wang CC, Kao TW, Chan JY, Yang YH, Chang YW, Chen WL. Relationship

578 between hyperuricemia and lipid profiles in US adults. Biomed Res Int. 2015;
579 2015:127596.
580 34. Zhang X, Meng Q, Feng J, Liao H, Shi R, Shi D, Renqian L, Langtai Z, Diao Y, Chen
581 X. The prevalence of hyperuricemia and its correlates in Ganzi Tibetan
582 Autonomous Prefecture, Sichuan Province, China. Lipids Health Dis. 2018;
583 17:235.
584 35. Sato A, Yamanaka H, Oe K, Yokoyama I, Yamazaki Y, Ebina K. Highly stable,
585 fluorescence-labeled heptapeptides substituted with a D-amino acid for the
586 specific detection of oxidized low-density lipoprotein in plasma. Chem Biol
587 Drug Des. 2015; 85:348-355.
588 36. Liu N, Sun Q, Xu H, Yu X, Chen W, Wei H, Jiang J, Xu Y, Lu W. Hyperuricemia
589 induces lipid disturbances mediated by LPCAT3 upregulation in the liver. Faseb
590 j. 2020; doi: 10.1096/fj.202000950R.
591 37. Kupke IR, Heller B, Weiss P, Zeugner S, Kather B, Wellern F. Early indicators for
592 the risk of atherogenesis. A field test of a new methodology on kindergarten
593 children in Düsseldorf. Atherosclerosis. 1983; 48:29-48.
594 38. Kang HH, Won KB, Heo R, Han D, Chang HJ. Independent association of serum
595 uric acid levels with arterial stiffness in the absence of established
596 cardiovascular disorders. Int J Clin Pract. 2020; doi: 10.1111/ijcp.13720.
597 39. Kuksis A, Marai L, Gornall DA. Direct gas chromatographic examination of total
598 lipid extracts. J Lipid Res. 1967; 8:352-358.
599 40. Sinnberg T, Lasithiotakis K, Niessner H, Schittek B, Flaherty KT, Kulms D, Maczey

E, Campos M, Gogel J, Garbe C, Meier F. Inhibition of PI3K-AKT-mTOR signaling sensitizes melanoma cells to cisplatin and temozolomide. J Invest Dermatol. 2009; 129:1500-1515.

41. Altman JK, Yoon P, Katsoulidis E, Kroczynska B, Sassano A, Redig AJ, Glaser H, Jordan A, Tallman MS, Hay N, Platanias LC. Regulatory effects of mammalian target of rapamycin-mediated signals in the generation of arsenic trioxide responses. J Biol Chem. 2008; 283:1992-2001.

42. Huang WH, Liu J, Zhang Q, Tang Y, Li M, Liu J, Liu JX. Effect of High Insulin on URAT1 Expression in Cultured HK-2 Cells and the Role of PI3K/Akt1 Pathway. Diabetes-Metabolism Research and Reviews. 2015; 31:23-24.

Figures

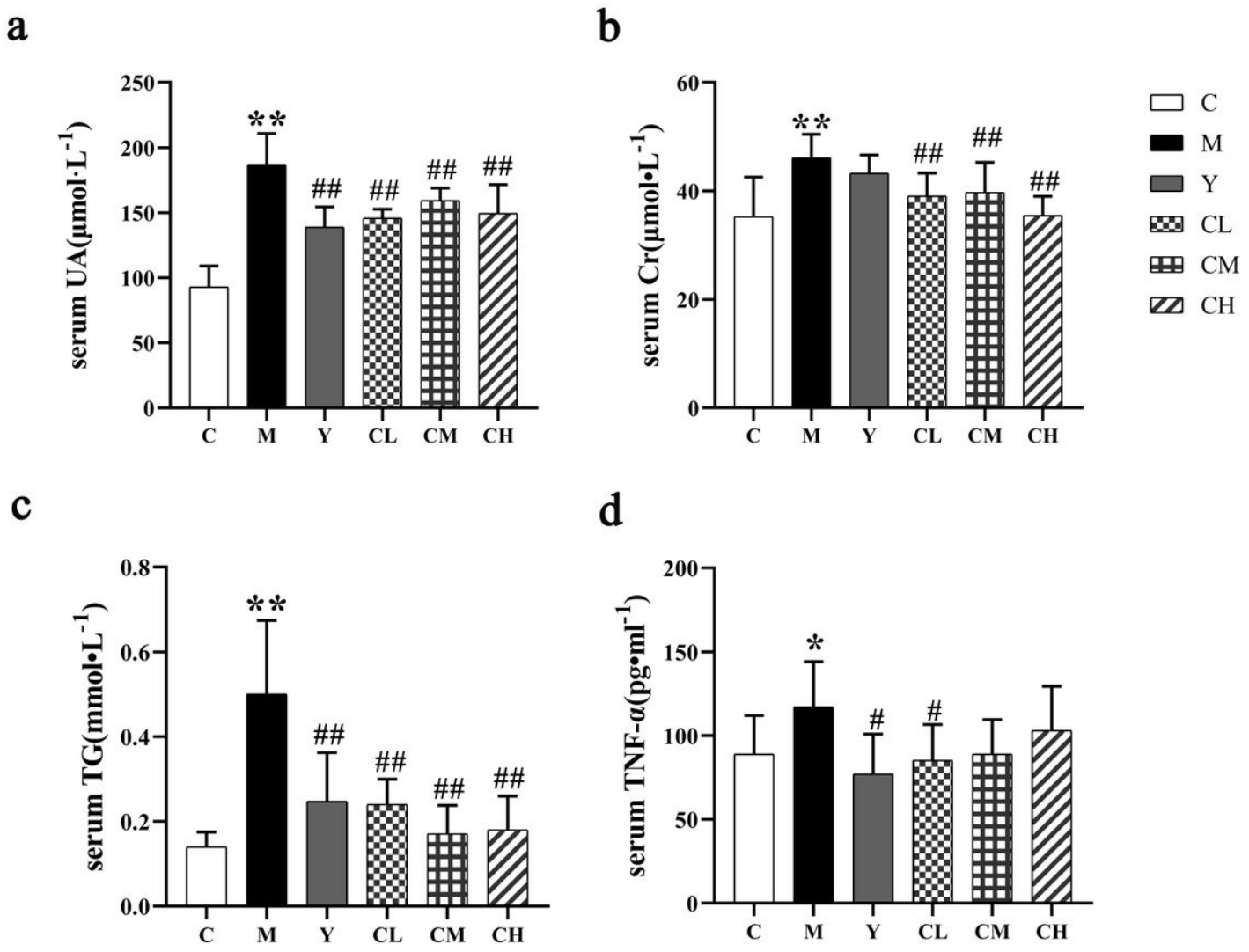

Figure 1

The levels of serum UA, Cr, TG, TNF-α in each group. C, control group; M, model group; Y, benzbromarone group; CL, low dosage group; CM, medium dosage group; CH, high dosage group; values are given as the mean ± SD (n=7), **, P<0.01 vs. control group. *, P<0.05 vs. control group; ##, P<0.01 vs. model group; #, P<0.05 vs. model group.

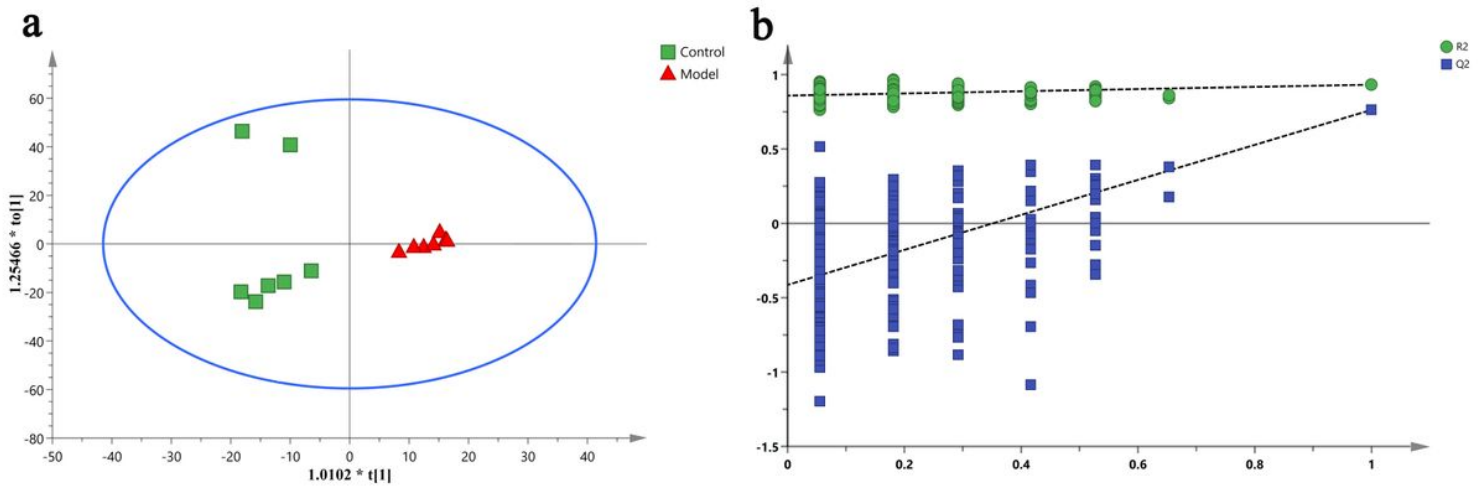

Figure 2

OPLS-DA score plots (a) and the corresponding validation plots (b) with 200 times permutation tests obtained.

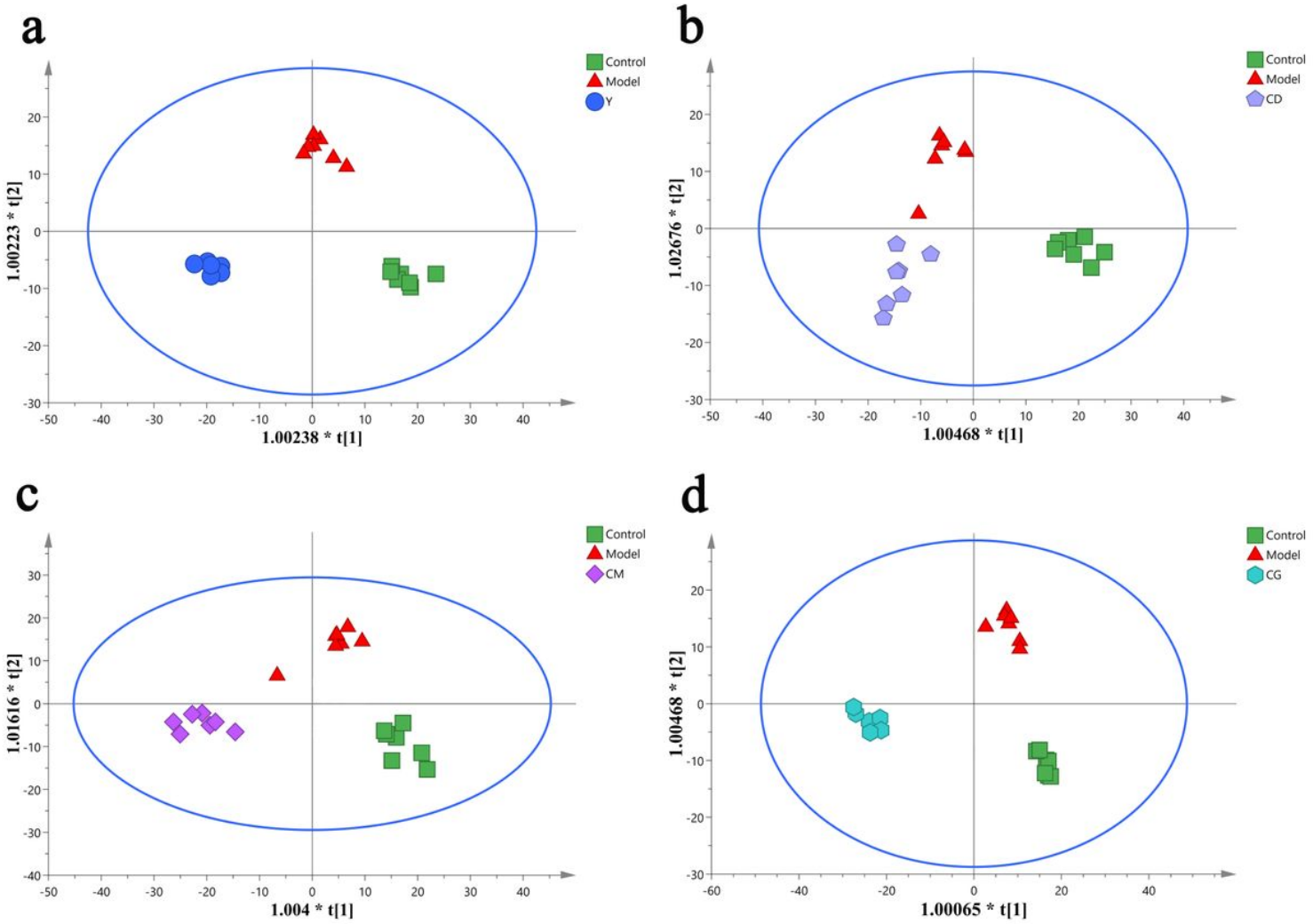

Figure 3

Metabolic profiles of rat serum in the control, model, benzbromarone, and different dose Plantaginis semen groups. C, control group; M, model group; Y, benzbromarone group; CL, low dosage group; CM, medium dosage group; CH, high dosage group.

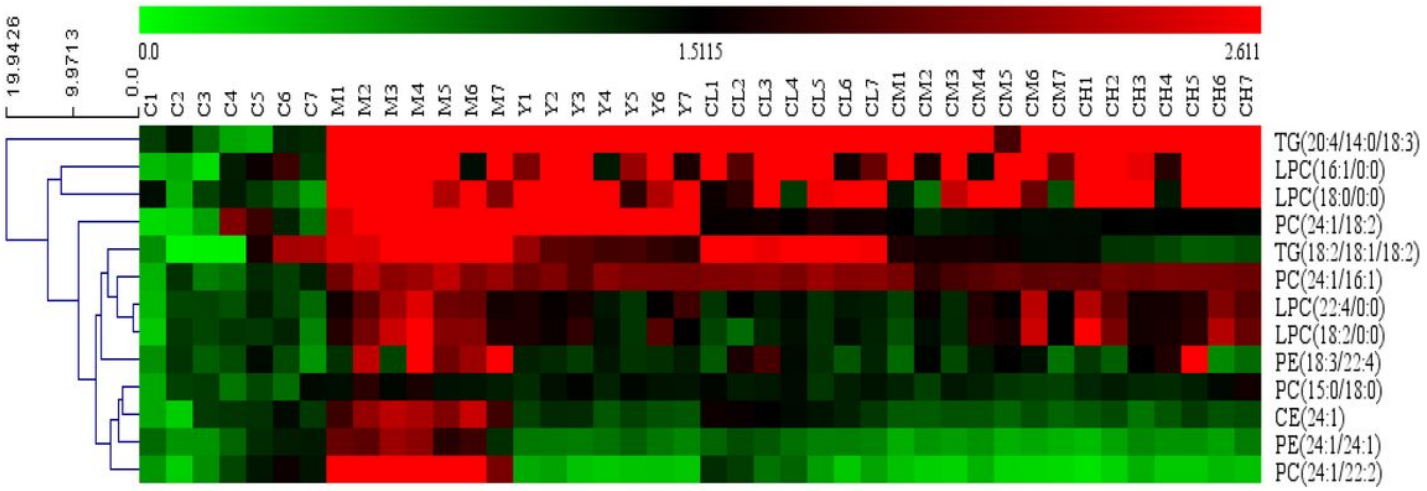

Figure 4

Heat map analysis of relative contents of potential metabolites. (green through dark red corresponding to a progressive increase in concentration). C, control group; M, model group; Y, benzbromarone group; CL, low dosage group; CM, medium dosage group; CH, high dosage group.

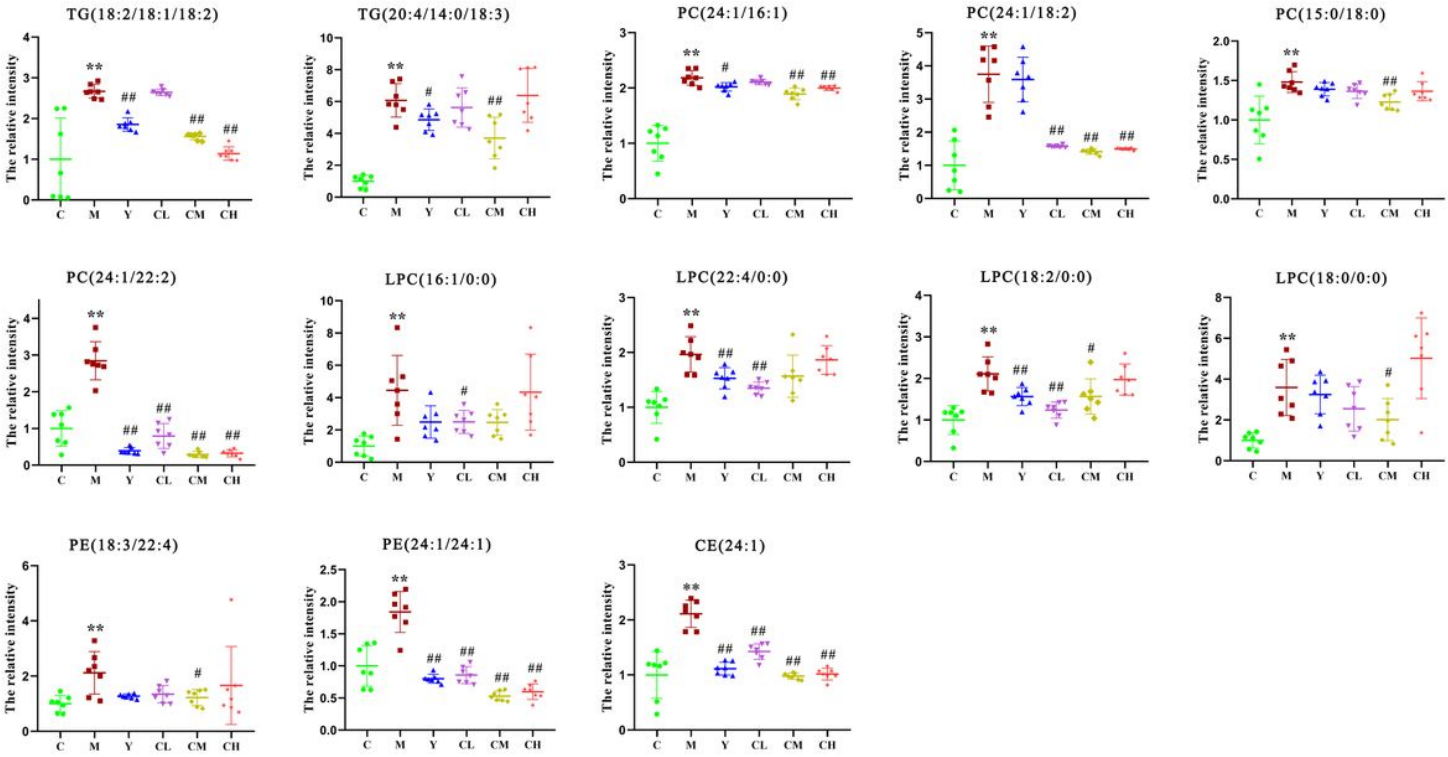

Figure 5

Comparison of 13 biomarkers peak relative signal intensities in 6 groups. The relative value of potential biomarkers in the control group was set as 1. C, control group; M, model group; Y, benzbromarone group; CL, low dosage group; CM, medium dosage group; CH, high dosage group; **, P<0.01 vs. control group. *, P<0.05 vs. control group; ##, P<0.01 vs. model group; #, P<0.05 vs. model group.

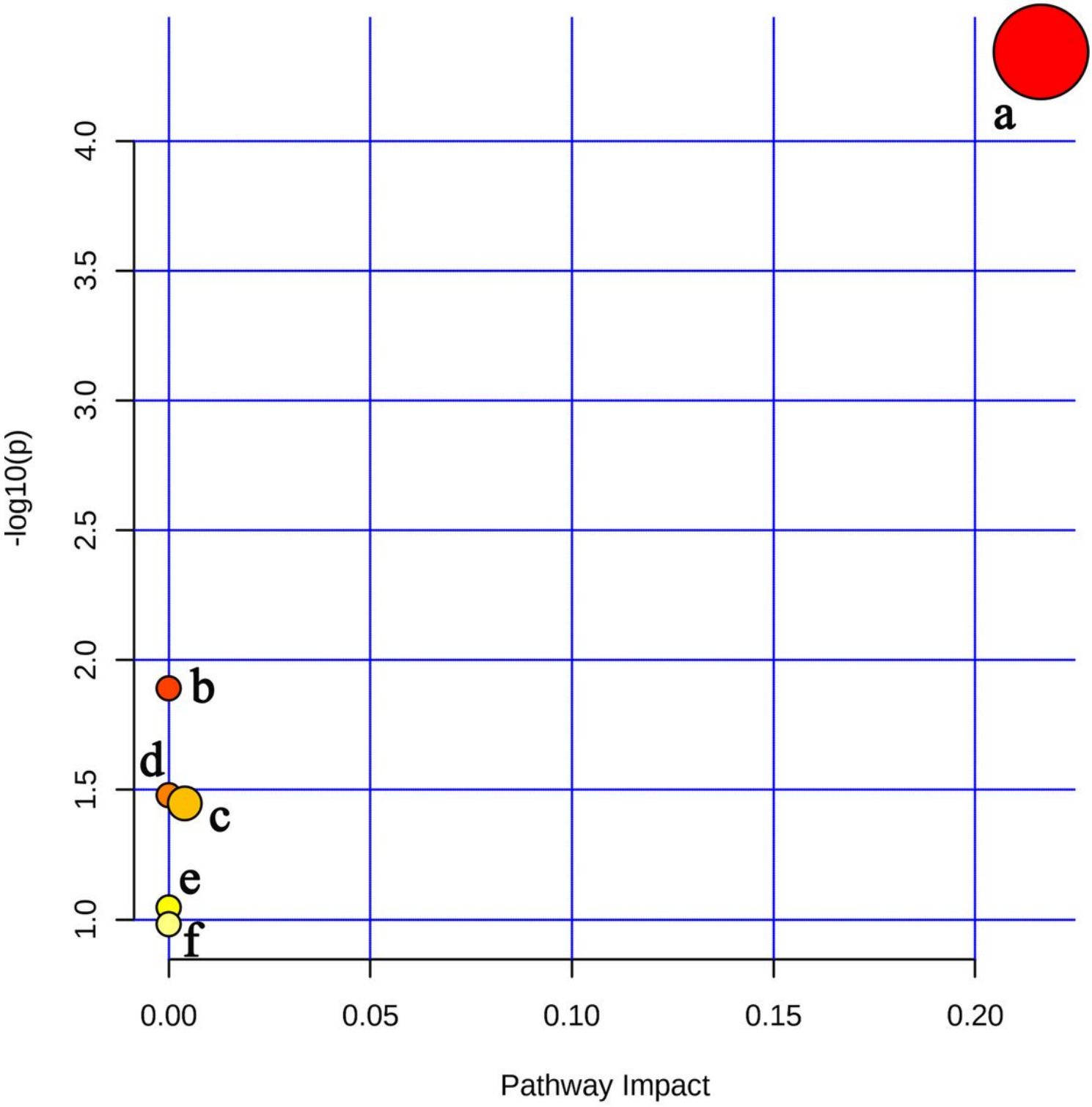

Figure 6

six pathway related to changed biomarkers. a: Glycerophospholipid metabolism, b: Linoleic acid metabolism, c: Glycosylphosphatidylinositol (GPI)-anchor biosynthesis, d: alpha-Linolenic acid metabolism, e: Arachidonic acid metabolism, f: Steroid biosynthesis.

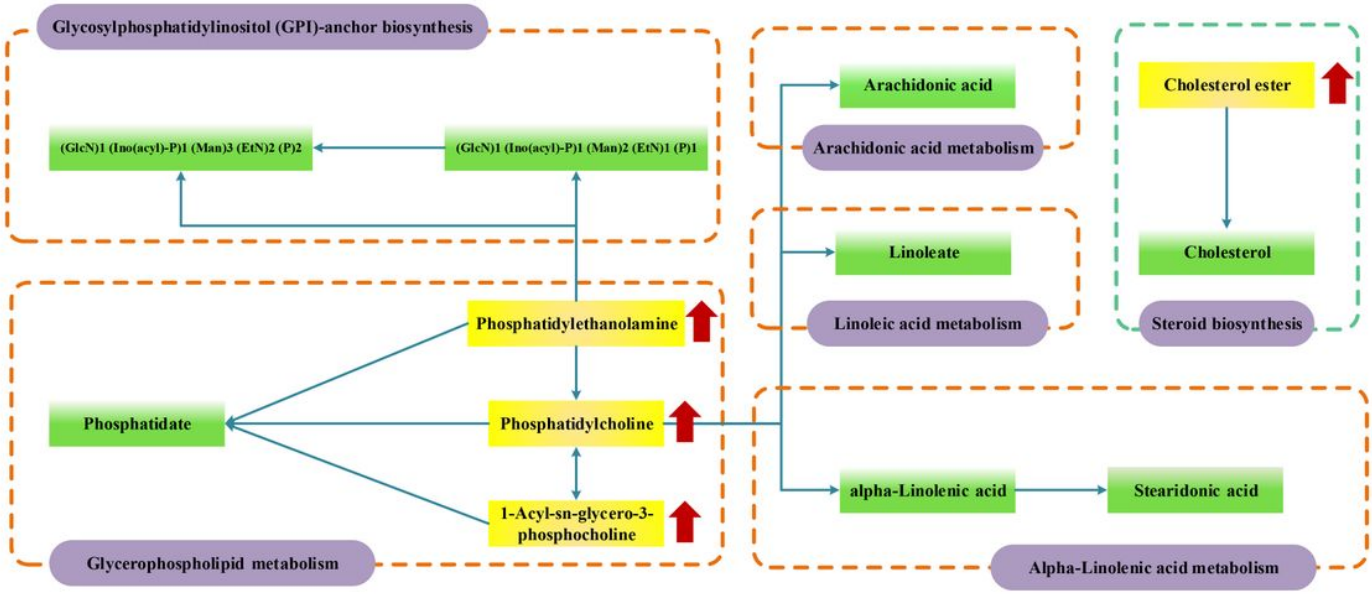

Figure 7

KEGG global metabolic network related to changed biomarkers. The purple textboxes represented the pathways, the yellow and green textboxes represented the significant and no detection metabolites. The arrows in red represented the up regulated metabolites. The arrows in blue represented direct or indirect connections between two metabolites.

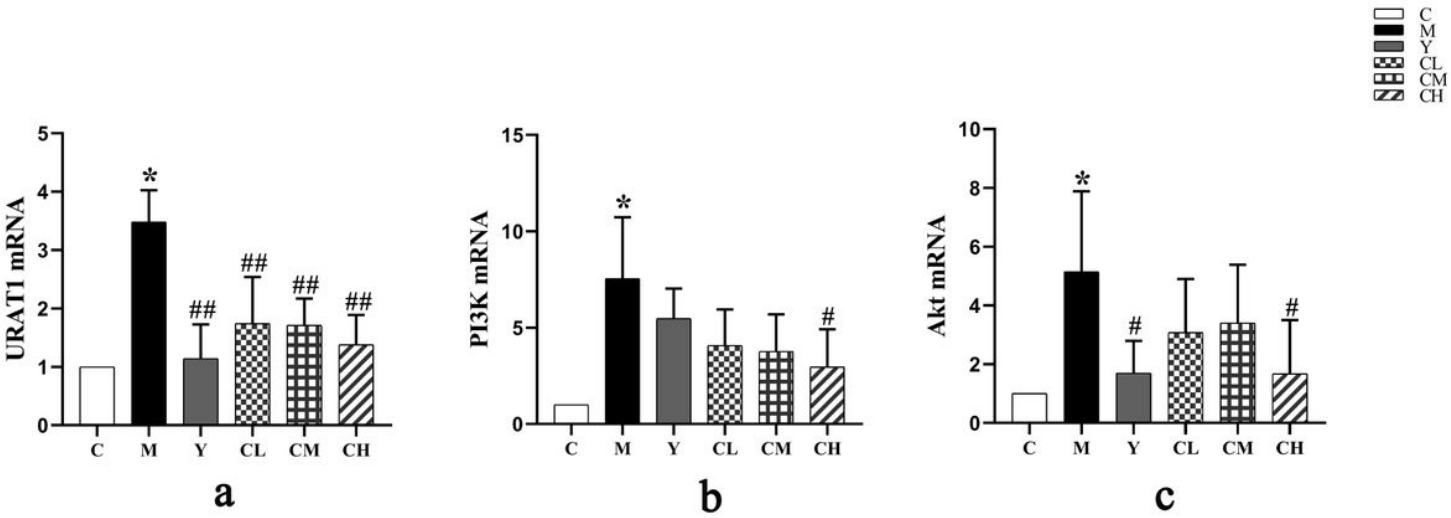

Figure 8

Effects of Plantaginis semen on PI3k/Akt and UTAR1 mRNA expression. C, control group; M, model group; Y, benzbromarone group; CL, low dosage group; CM, medium dosage group; CH, high dosage group; values are given as the mean ± SD(n=7), **, P<0.01 vs. control group. *, P<0.05 vs. control group; ##, P<0.01 vs. model group; #, P<0.05 vs. model group.